Aerosol and Air Quality Research, 19: 2697–2706, 2019

ISSN: 1680-8584 print / 2071-1409 online
doi: 10.4209/aaqr.2019.07.0368

Seasonal Characteristics of Sulfate and Nitrate in Size-segregated Particles in Ammonia-poor and -rich Atmospheres in Chengdu, Southwest China

Qinkai Li[1,2], Zhou Yang[3], Xiaodong Li[1,2*], Shiyuan Ding[1,2], Feng Du[4]

[1] *Institute of Surface-Earth System Science, Tianjin University, Tianjin 300072, China*
[2] *Tianjin Key Laboratory of Earth Critical Zone Science and Sustainable Development in Bohai Rim, Tianjin University, Tianjin 300072, China*
[3] *College of Tourism and Geographical Sciences, Tongren University, Tongren 565300, China*
[4] *State Key Laboratory of Geohazard Prevention and Geoenvironment Protection, Chengdu University of Technology, Chengdu 610059, China*

ABSTRACT

In order to determine the seasonal characteristics of water-soluble inorganic ions (WSIIs) in aerosols in urban atmospheres, size-segregated particulate matter (PM) samples were collected over a one-year period from February 2012 to January 2013 in a typical urban location, Chengdu in Southwest China, using an Andersen cascade impactor sampler. The PM mass concentrations, particularly the fine fraction, peaked during winter, and the WSIIs were more enriched in the fine fraction (21.7%) than the coarse fraction (9.2%). The sums of the equivalent ratios of cations (Na^+, NH_4^+, K^+, Mg^{2+}, and Ca^{2+}) to anions (SO_4^{2-}, NO_3^-, Cl^-, and F^-) indicated that the fine particles (0.86) were more acidic than the coarse ones (1.60). The average NH_4^+/SO_4^{2-} molar ratio (A/S) in the fine fraction (1.79) was much higher during winter than the other three seasons (< 1.5), implying a generally NH_3-poor atmosphere in Chengdu; hence, the NO_3^- in the fine particles was principally formed through homogeneous reactions involving ammonia and nitric acid during winter, whereas it was heterogeneously formed during the other three seasons. Significant positive correlations were observed between the A/S and NO_3^- molar concentrations during spring and winter; therefore, the formation of particle-phase NO_3^- may be accelerated by increased A/S in both NH_3-poor and -rich atmospheres. Moreover, the A/S and NO_3^-/SO_4^{2-} molar ratios displayed negative and positive correlations during spring and winter, respectively, suggesting that the variation in atmospheric NH_4^+ (or NH_3) during winter affected the formation of NO_3^- more strongly than that of SO_4^{2-}, whereas more SO_4^{2-} than NO_3^- was formed in the NH_3-poor atmosphere during spring, when most of the NO_3^- in the aerosols would be expected to form via heterogeneous reactions.

Keywords: Size-segregated particles; Sulfate; Nitrate; Ammonium; Chengdu.

INTRODUCTION

Atmospheric particulate matter (PM) is one of the most important components that could affect the air quality, climate change and public health (IPCC, 2013; WHO, 2013). Over last few decades, researches have been carried out in many studies worldwide, focusing on the sources and secondary formation and transformation mechanisms of PM and its effects on human health and the earth radiation balance (Seinfeld and Pandis, 1998; Dockery *et al.*, 1993; Huang *et al.*, 2014; Wang *et al.*, 2016; Yao *et al.*, 2018). Atmospheric PM can be derived from both anthropogenic and natural sources, and can also be formed in the atmosphere from secondary processes (oxidation of gaseous species), and the particle size ranges from a few nanometers to several tens of micrometers (Zhang *et al.*, 2015; Wang *et al.*, 2017a) that plays a critical role in their environmental and human health effects (Kulmala *et al.*, 2004; West *et al.*, 2016; Tian *et al.*, 2018; Klimont *et al.*, 2017).

The water-soluble inorganic ions (WSIIs) including anions (SO_4^{2-}, NO_3^-, Cl^- and F^-) and cations (Ca^{2+}, Mg^{2+}, Na^+, K^+ and NH_4^+), often account for a major fraction of atmospheric PM mass, play a vital role in scattering incoming solar radiation and altering cloud properties and thus enhance the indirect radiative forcing (Seinfeld and Pandis, 1998; Zhao *et al.*, 2011). Recent studies have indicated that the WSII fraction in PM varies not only with time and space but also with the particle size, which could provide key information for interpreting the sources and formation mechanisms of the PM (Zhang *et al.*, 2008; Huang *et al.*, 2016; Wu *et al.*, 2017). To a large extent, WSIIs determines the particle acidity and hygroscopicity, which could control the rates of

* Corresponding author.
Tel.: +86 022-83614909; Fax: +86 022-27405053
E-mail address: xiaodong.li@tju.edu.cn

heterogeneous chemical reactions (He *et al.*, 2012; Hennigan *et al.*, 2015; Wang *et al.*, 2016; Weber *et al.*, 2016; Tian *et al.*, 2018). In general, the SO_4^{2-}, NO_3^- and NH_4^+ (together called *SNA*) are dominant WSIIs in fine-mode PM and exist primarily in the forms of $(NH_4)_2SO_4$, NH_4HSO_4 and NH_4NO_3 and expected to be formed through the neutralization reactions between acids (i.e., H_2SO_4 and HNO_3) and NH_3 in gas phase (Yao *et al.*, 2002; Lin *et al.*, 2006; Lin and Cheng, 2007; Wu *et al.*, 2018). As NH_3 could neutralize the H_2SO_4 to $(NH_4)_2SO_4$ or NH_4HSO_4 (Wang *et al.*, 2005; Vieira-Filho *et al.*, 2016), the NH_4^+/SO_4^{2-} (A/S) molar ratio of 1.5 can be considered as an indicator in determining the formation pathways of NO_3^- in the atmosphere (Pathak *et al.*, 2004, 2009). In "excess NH_4^+" (i.e., A/S > 1.5, NH_3-rich) environment, NO_3^- is supposed to be formed homogeneously whereas in "deficient NH_4^+" (i.e., A/S < 1.5, NH_3-poor) environment, it tends to be formed via heterogeneous reactions, the NH_3 is insufficient to neutralize the HNO_3 (He *et al.*, 2012; Behera *et al.*, 2013; Tian *et al.*, 2018). However, the current available studies on A/S values focused mainly on fine-mode particles, since the NH_4^+ could be of less importance on coarse particles (Wu *et al.*, 2017; Jiang *et al.*, 2019). Recently, atmospheric NH_3 has become a public concern for its potential in facilitating the formation of secondary aerosol, but it is yet to be regulated in many regions around the world. Therefore, to better understand the formation of SO_4^{2-} and NO_3^- in both fine and coarse PM, long-term observations of WSIIs in PM is necessary, despite the recent progress, including their seasonal characteristics, which could help in identifying the PM sources and elucidating the transformation mechanisms of heavy haze formation over megacities in China (Wang *et al.*, 2017b; Zou *et al.*, 2018).

Chengdu, the capital city of Sichuan Province, is located at the western part of the Sichuan Basin. Due to the blocked terrain and relatively stagnant weather in Sichuan Basin, the pollutants emitted from local sources are retained for longer time compared to the other areas of China, and frequently results heavy air pollution (haze) events at Chengdu (Ning *et al.*, 2018). Besides, the increase in energy consumption due to rapid industrialization and urbanization over the past few decades should be significantly contributing to the severe urban haze in Chengdu. However, the studies on characterization of PM and the sources of haze in Chengdu are limited to short-term observations (e.g., the dust and biomass burning) and model simulations (Chen and Xie, 2013; Tao *et al.*, 2013; Tian *et al.*, 2013; Wang *et al.*, 2013b; Tao *et al.*, 2014; Chen *et al.*, 2015; Shi *et al.*, 2017). In this study, we focused on identification of PM sources through the measurements of major WSIIs in size-segregated particles collected over a one-year period in Chengdu, Southwest China. We discuss the seasonal characteristics and formation mechanisms of aerosol SO_4^{2-} and NO_3^- in the NH_3-poor and -rich atmosphere at Chengdu.

MATERIALS AND METHODS

Study Location

Chengdu is situated in Sichuan Basin with the Qinghai-Tibet Plateau on the west, Qinling Mountains and the Loess Plateau on the north, Hunan and Hubei Province on the east, and the Yunnan-Guizhou Plateau on the south. The climate of Sichuan Basin is characterized by subtropical monsoon and temperate oceanic climate (Chen and Xie, 2014; Li *et al.*, 2015). The weather is categorized into four distinct seasons with the temperature ranging from 5°C in winter to 26°C in summer. Average annual precipitation is 918 mm with high abundance and frequency in summer to autumn (i.e., from June to November) period than in winter to spring (i.e., from December to May).

As one of the most crowded regions in Sichuan Basin, Chengdu has a permanent population of more than 14 million, and the population density is about 964 people per square kilometer. Like many other megacities in China, Chengdu is growing at an unprecedented pace with an urbanization rate of 60.2% in 2012, and it had the eighth largest gross domestic production in China. According to the statistical yearbook of Chengdu for 2013 (Chengdu Bureau of Statistics), the total vehicle number exceeded 3.0 million by the end of 2012, which is the second highest number among all Chinese cities. The industrial areas are mostly located in the northern suburbs of city, about 20 km away from the sampling site. The total energy consumption of Chengdu increased from 24 million tons of standard coal equivalent to 44.4 million tons of standard coal equivalent between 2005 and 2012, according the statistics from the World Resources Institute (http://www.wri.org).

Sampling

Size-segregated atmospheric particle sampling was performed using an eight-stage Andersen cascade impactor air sampler (AN-200; SIBATA, Japan) in Chengdu, Southwest China. The sampler was placed on the rooftop of a building (15 m above ground level) in Chengdu University of Technology (CDUT) campus (30°40′40″N, 104°08′30″E), located at Chenghua district in the urban northeastern part of Chengdu. The cut points of the sampler were set as 11, 7.0, 4.7, 3.3, 2.1, 1.1, 0.65 and 0.43 μm, and the samples were collected from 15 February 2012 to 21 January 2013 at flow rate of 28.3 L min^{-1} with a frequency of 4–8 days for each sample, in order to ensure adequate particle load for reliable chemical analysis. Before sampling, the quartz fiber filters (Ø80 mm, Tissuquartz 2500QAT-UP; Pallflex) were preheated in a muffle furnace at 450°C for 6 h, and wrapped in aluminum foil individually after sampling, then sealed in airtight polyethylene bags and stored at –18°C until analysis. In this study, a total of 108 filter samples were obtained, and field blanks were sampled without sucking air for 10 min and treated the same way as particle samples.

Chemical and Statistical Analyses

Filters were gravimetrically weighed before and after the sampling, after 24 h equilibration at constant temperature (20–23°C) and relative humidity (35–45%), using a Sartorius MC5 electronic microbalance with a sensitivity of ±1 μg (Sartorius; Göttingen, Germany). The weight difference between before and after sampling was considered as particle weight and the mass concentration was calculated by dividing it with the sample air volume.

Half of the sample filters was cut into pieces, soaked in

15 mL deionized water (18.2 MΩ; Milli-Q, USA) and ultrasonically extracted three times (i.e., 10 min each). After the extraction, the solutions were then filtered through syringe filters (0.22 μm; Millipore) and stored in high-density polyethylene bottles for subsequent WSII analysis. Anions (F^-, Cl^-, NO_3^- and SO_4^{2-}) and cations (Na^+, K^+, Ca^{2+} and Mg^{2+}) were measured using ion chromatography (ICS-90; Dionex, USA) and inductively coupled plasma optical emission spectrometry (ICP-OES; MPX, USA), respectively, and the NH_4^+ was measured with a SKALAR continuous flow analyzer (San^{++} Automated Wet Chemistry Analyzer; Holland). The instrument detection limits are 0.02 mg L^{-1} for anions and 0.005 mg L^{-1} for cations and NH_4^+ (Xiao and Liu, 2004; Yang *et al.*, 2015). Standard reference materials produced by the National Institute of Metrology in China were used for quality assurance, and the measurement uncertainties for different ion concentrations in this study were typically less than 5% based on replicate analysis of standards. No targeted ions were detected in the field blank.

To compare the results obtained in size-segregated particles among the four seasons, Student's *t*-test was performed by assuming equal variance in two populations at a 95% confidence level with SPSS Statistics (version 19.0; IBM Corp., Armonk, NY, USA). Correlation analysis was also performed among concentration data and molar data across the study period. Statistically significant difference was set at *p* values less than 0.05 unless otherwise stated.

RESULTS AND DISCUSSION

Aerosol Particle Mass Concentrations

Since the Anderson impactor sampler does not have a 2.5 μm cut point, the diameter of 2.1 μm is defined as the boundary for fine and coarse particles in this study (Fig. 1). The annual mean concentrations of $PM_{2.1}$ and PM_{11} are 125.9 ± 56.1 μg m^{-3} and 224.5 ± 83.6 μg m^{-3}, respectively. They were significantly higher than the annual $PM_{2.5}$ and PM_{10} limits of both Chinese National Ambient Air Quality Standards (35 and 70 μg m^{-3}; Grade II of GB3095-2012) and the WHO air quality guidelines (10 and 20 μg m^{-3}; WHO, 2006). Nevertheless, these values are comparable with other studies synchronously conducted at Chengdu (120.4 and 195.5 μg m^{-3}), but higher than those reported at Wuhan (89.6 and 134.9 μg m^{-3}), Shanghai (103.1 and 149.2 μg m^{-3}), and Guangzhou (97.5 and 144.4 μg m^{-3}) and lower than those reported at Xi'an (140.9 and 257.8 μg m^{-3}) over the parallel periods (Wang *et al.*, 2006; Shi *et al.*, 2017; Wang *et al.*, 2013a; Wang *et al.*, 2015; Wang *et al.*, 2017c), indicating that the PM loading is high at Chengdu.

The PM_{11} mass concentration peaked in March (378.4 μg m^{-3}) followed by February (371.4 μg m^{-3}). However, the $PM_{2.1}/PM_{11}$ ratio was significantly higher in February (0.70) than that in March (0.54) (Fig. 1), despite the fact that the PM_{11} mass concentration was comparable, implying that the sources and/or formation pathways of the PM were different in these two months (Tao *et al.*, 2013; Wang *et al.*, 2013b; Chen *et al.*, 2015). An increase trend of the $PM_{2.1}/PM_{11}$ ratio was observed during the campaign from spring to winter, except for two anomalous high values in May and July, which might be caused by the crop residue burning around Chengdu (Tao *et al.*, 2013; Chen and Xie, 2014). Seasonally, the $PM_{2.1}/PM_{11}$ ratio in winter (0.65 ± 0.04) is significantly higher than that in the other three seasons, which might be caused by the enhanced emission from anthropogenic activities (e.g., bulk coal and biomass burning for civil heating) and poor air diffusion condition due to low temperature and wind speed, which promote the fine particles' formation and accumulation (Table 1) (Ning *et al.*, 2018).

Size Distribution of WSIIs

Total WSIIs of $PM_{2.1}$ ranged from 10.5 to 68.9 μg m^{-3}, with an annual average of 27.6 ± 19.8 μg m^{-3}, and accounted for 20.7% of the $PM_{2.1}$ mass, whereas the annual average of WSIIs

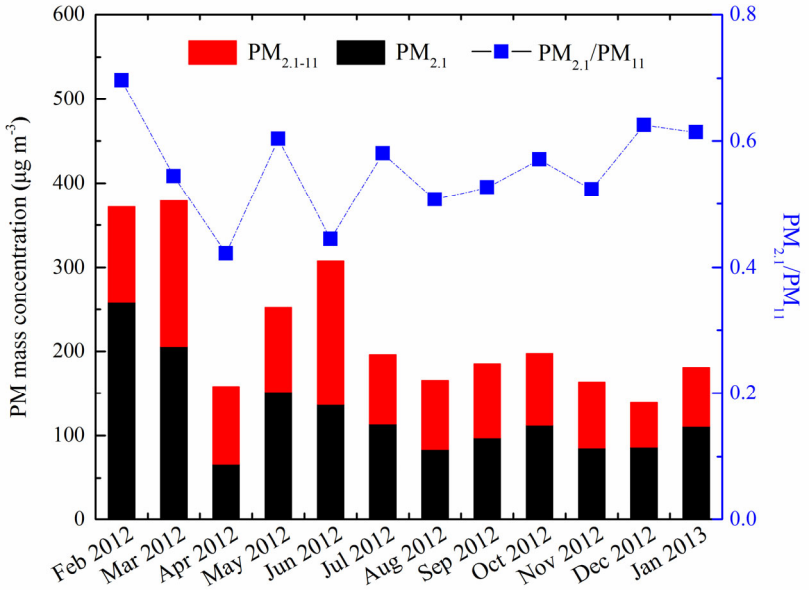

Fig. 1. Time series of $PM_{2.1}$ and $PM_{2.1\text{-}11}$ mass concentrations and $PM_{2.1}/PM_{11}$ mass ratios.

Table 1. Meteorological records during each sampling month.

Sampling periods	T[a] (°C)	RH[b] (%)	WS[c] (km h^{-1})	P[d] (hPa)	Visibility (km)
15–21 Feb 2012	6.57 ± 1.4	81.0 ± 5.5	5.4 ± 3.3	1021.0 ± 4.6	3.6 ± 0.5
11–19 Mar 2012	14.0 ± 3.4	67.2 ± 5.1	4.4 ± 1.1	1011.4 ± 5.8	4.8 ± 1.1
11–18 Apr 2012	18.1 ± 1.0	62.8 ± 9.3	7.0 ± 2.1	1009.0 ± 1.5	7.6 ± 2.0
14–18 May 2012	23.4 ± 1.8	53.2 ± 7.0	5.0 ± 2.1	1007.6 ± 3.6	7.2 ± 2.4
18–23 Jun 2012	24.0 ± 1.7	79.5 ± 7.6	2.7 ± 0.5	1002.8 ± 2.1	4.2 ± 1.6
15–22 Jul 2012	24.1 ± 1.7	88.0 ± 3.9	4.6 ± 1.9	1003.3 ± 2.1	5.1 ± 1.8
15–22 Aug 2012	27.1 ± 2.5	74.4 ± 8.9	5.9 ± 1.6	1006.1 ± 3.5	8.1 ± 1.5
13–18 Sep 2012	19.3 ± 1.9	81.8 ± 11.4	5.3 ± 2.6	1014.5 ± 1.4	4.6 ± 1.5
9–15 Oct 2012	18.3 ± 1.4	90.0 ± 5.5	3.3 ± 2.8	1015.3 ± 3.1	4.7 ± 0.8
15–24 Nov 2012	12.2 ± 1.6	68.8 ± 10.5	4.6 ± 1.4	1014.9 ± 4.2	6.2 ± 2.4
9–17 Dec 2012	9.67 ± 0.7	85.0 ± 6.4	4.1 ± 1.4	1015.0 ± 3.1	3.1 ± 1.3
15–21 Jan 2013	7.57 ± 0.5	77.3 ± 9.5	4.6 ± 1.8	1019.4 ± 5.8	3.1 ± 1.4

The meteorological data can be found at https://www.wunderground.com/. [a] Temperature; [b] Relative Humidity; [c] Wind Speed; [d] Sea-level Pressure.

in $PM_{2.1\text{-}11}$ was 9.6 ± 7.6 μg m^{-3} (range: 4.4–28.6 μg m^{-3}) and accounted for about 9.2% of $PM_{2.1\text{-}11}$, which indicates that the WSIIs are highly enriched in fine particles. Furthermore, the total WSIIs in $PM_{2.1}$ was the highest in winter (40.5 ± 24.8 μg m^{-3}), followed by spring (39.6 ± 22.9 μg m^{-3}), summer (17.4 ± 7.5 μg m^{-3}) and autumn (12.7 ± 0.9 μg m^{-3}), while the WSIIs in $PM_{2.1\text{-}11}$ was higher in spring (16.9 ± 10.2 μg m^{-3}), followed by winter (10.0 ± 9.4 μg m^{-3}), summer (6.3 ± 1.8 μg m^{-3}) and autumn (5.1 ± 0.4 μg m^{-3}). It is noteworthy that the total WSIIs in both fine and coarse particles reduced sharply in summer and autumn at Chengdu that can be attributed largely to high rainfall during monsoon seasons (Xiao and Liu, 2004; Pan *et al.*, 2017). The content of WSIIs in fine fraction in winter is comparable to that in spring, whereas in coarse fraction, it was significantly higher in spring than that in winter, suggesting their enhanced contribution from biomass burning and/or dust storms in spring (Tao *et al.*, 2013; Wang *et al.*, 2013b; Chen *et al.*, 2015; Tian *et al.*, 2016; Shi *et al.*, 2017). The abundances of WSIIs in $PM_{2.1}$ were: $SO_4^{2-} > NO_3^- > NH_4^+ > Cl^- > Mg^{2+} > K^+ > Ca^{2+} > Na^+ > F^-$, while in $PM_{2.1\text{-}11}$ they were: $SO_4^{2-} > Ca^{2+} > NO_3^- > Cl^- > NH_4^+ > Mg^{2+} > K^+ > Na^+ > F^-$ (Table 2), indicating that SO_4^{2-} and NO_3^- are dominant species in PM at Chengdu. The discrepancies in the order of major ions' abundances in fine and coarse fractions might have been driven by the differences in their formation pathways (Li and Shao, 2009; Liu *et al.*, 2015; Li *et al.*, 2018). Generally, SO_4^{2-}, NO_3^-, and NH_4^+ are formed by chemical reactions between the gas-phase precursors such as NO_x, SO_2, and NH_3 in the atmosphere, however, the relatively high abundances of SO_4^{2-}, Ca^{2+}, and NO_3^- and low abundance of NH_4^+ in the coarse fraction indicate that they were mostly formed through heterogeneous reactions of the gas-phase precursors on pre-existing particles and/or derived from soil dust (Lin and Cheng, 2007; Tao *et al.*, 2013; Chen *et al.*, 2015; Shi *et al.*, 2017).

Size distributions of major ions in each season are plotted as dC/dlogDp as a function of Dp (diameter of particles) and showed in Fig. 2. SO_4^{2-} showed a unimodal distribution with a peak at 0.65–1.1 μm. SO_4^{2-} can be directly emitted into the atmosphere from primary sources like burning processes and

Table 2. The mean and S.D. of WSIIs' mass concentrations in $PM_{2.1}$ and $PM_{2.1\text{-}11}$.

WSIIs (μg m^{-3})	$PM_{2.1}$		$PM_{2.1\text{-}11}$	
	Mean	S.D.[a]	Mean	S.D.
SO_4^{2-}	13.2	9.76	3.22	2.78
NO_3^-	6.08	4.17	1.91	1.65
Cl^-	1.58	1.21	0.61	0.33
F^-	0.01	0.02	0.15	0.19
Ca^{2+}	0.56	0.21	2.15	1.54
Mg^{2+}	0.92	1.66	0.45	0.92
Na^+	0.30	0.47	0.19	0.25
K^+	0.90	0.50	0.35	0.15
NH_4^+	4.01	4.39	0.58	0.82

[a] S.D.: Standard Deviation.

can also be produced in the atmosphere by homogeneous oxidation reactions of reduced sulfur species (e.g., SO_2 or DMS) with OH radical, H_2O_2 and ozone (Seinfeld and Pandis, 1998; Guo *et al.*, 2010). On the other hand, it can also be formed by heterogeneous reactions including the aqueous-phase reactions (e.g., cloud processes) (Guo *et al.*, 2010; Huang *et al.*, 2018). In spring, in addition to a major peak at 0.65–1.1 μm, SO_4^{2-} showed two minor peaks at 2.1–4.7 and 7.0–11 μm, which indicate that it should have been significantly produced by both homogeneous and heterogeneous reactions in Chengdu (Zhuang *et al.*, 1999). Interestingly, NO_3^- showed unimodal distribution in warm (i.e., spring and summer) and bimodal distribution in cold (autumn and winter) periods (Fig. 2(b)). Such differences imply that NO_3^- sources and/or formation processes might be different during warm and cold periods in Chengdu. NO_3^- can be formed more favorably through gas-to-particle conversion at lower temperature, and it might also under the influence of sand storms occurred during dry seasons. In addition, contrary to SO_4^{2-}, NO_3^- showed a larger peak in winter than that in spring. In fact, ambient temperature and relative humidity are quite different during spring and winter, which might have greatly impacted their transformation mechanisms (Huang *et al.*, 2018). Aerosol NH_4^+ is generally formed from the alkaline gas (i.e., NH_3) by reacting with acidic species

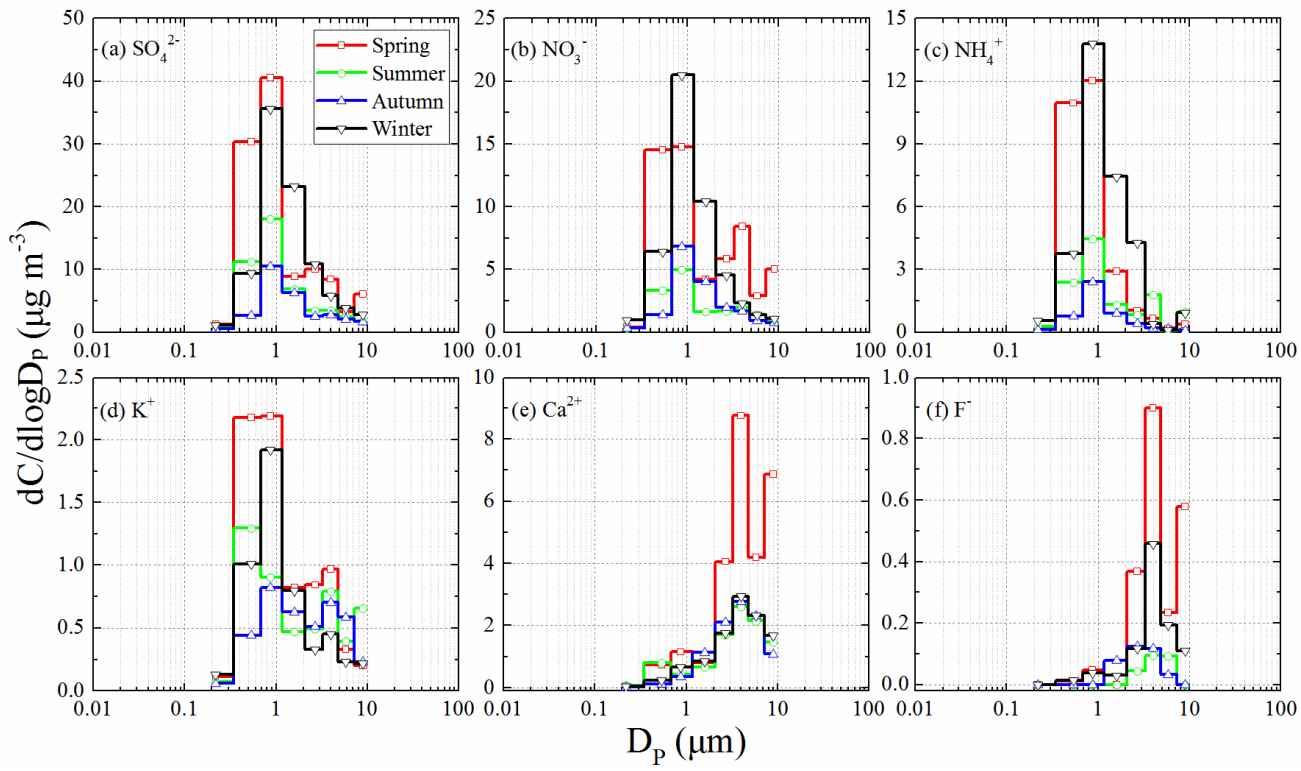

Fig. 2. The distributions of major WSIIs over four seasons, which showed dC/dlogDp value as a function of Dp (diameter of particles). The included WSIIs are: (a) SO_4^{2-}, (b) NO_3^-, (c) NH_4^+, (d) K^+, (e) Ca^{2+}, and (f) F^-.

(e.g., H_2SO_4, HNO_3 and HCl). It was largely enriched in fine-mode particles and peaked at 0.65–1.1 μm, consistent with SO_4^{2-} and NO_3^- (Fig. 2(c)), suggesting that NH_4NO_3, $(NH_4)_2SO_4$ and/or NH_4HSO_4 are the main forms of these ions in Chengdu PM (Wang *et al.*, 2013b; Huang *et al.*, 2016). The seasonal distributions of NH_4^+ could mainly be affected by the meteorological conditions. For example, ambient temperature can impact both the release of NH_3 and NH_4^+ phase portioning, and wet deposition of NH_4^+ should be significant in summer and autumn due to high rainfall, whereas in winter, the conversion and accumulation of NH_4^+ might be exacerbated due to low temperature and wind speed and frequent fog events (Pan *et al.*, 2017; Ning *et al.*, 2018).

K^+ showed bimodal distribution with a large peak in fine particles and exhibited the highest abundance in spring (Fig. 2(d)), probably due to enhanced biomass burning emissions. Generally, the particle K^+ is regarded as a good tracer for biomass burning emission into the atmosphere. Chen and Xie (2014) reported high concentrations of fine-mode K^+ during biomass burning episode occurred in spring at urban Chengdu. While during other seasons, it can be inferred that the fumes of biomass burning by domestic use (e.g., daily cooking) at rural areas are responsible for the fine-mode K^+. Ca^{2+} showed a bimodal distribution with the peaks in coarse-mode particles (3.3–4.7 and 7.0–11.0 μm) in each and every season (Fig. 2(e)), and showed extremely high loading in spring, which can be attributed for local fugitive dust due to the strong winds (Table 1) as well as long-range transported dust sands from arid or semi-arid areas of North China (Tao *et al.*, 2013). Resuspension of soil dust, marine aerosols, and material from volcanic eruptions are the major natural pathways of particle F^- entering the atmosphere, while aluminum smelting, coal combustion and brick manufacturing are its main anthropogenic sources (Carpenter, 1969; Kalinić *et al.*, 1997). A recent study also showed that biomass burning could be one of the major sources of fine particle F^- (Jayarathne *et al.*, 2014). Interestingly, the size distribution of F^- was similar to that of Ca^{2+}, i.e., peaked at 3.3–4.7 and 7.0–11.0 μm in spring (Fig. 2(f)). Such size distribution indicates that they were probably derived from the common source, such as the local fugitive cement dust, and the gaseous hydrogen fluoride emitted from combustion sources might heterogeneously react with coarse-mode Ca^{2+}. However, it is difficult to provide a definite conclusion from this study due to limited data, a subject of future research.

Particle Acidity in Urban Chengdu

Particle acidity is an important parameter that could influence the concentration, chemical composition, and toxicity of PM (Weber *et al.*, 2016). Nevertheless, direct measurement of particle acidity is difficult because of its low water content and nanoscale particle size, thus proxy methods and parameters, such as the in situ acidity, strong acidity and ion-balanced acidity are used for its estimation (Zhang *et al.*, 2008; He *et al.*, 2012; Kerminen *et al.*, 2001; Tian *et al.*, 2018). Recently, Tian *et al.* (2018) reported that charge equivalent ratio between measured cations to anions ($R_{CE/AE}$) is a good measure of acidity in fine-mode aerosol, because the temporal trend between $R_{CE/AE}$ and in situ pH was observed to be similar. He *et al.* (2012) also used the

equivalent charge ratio and showed similar seasonal variation in in situ $PM_{2.5}$ acidity and $R_{CE/AE}$, and the field observations have showed a general higher particle acidity in South China than North China. Moreover, an investigation conducted in four major cities of China by calculating the equivalent ratio of NH_4^+ to the sum of SO_4^{2-} plus NO_3^- during summertime indicated that the particle acidity was mostly dependent on the environmental SNA abundance (Pathak *et al.*, 2009).

In this study, we estimated the particle acidity by calculating $R_{CE/AE}$ in both sums of fine- and coarse-mode particles, and the results indicated that the fine particles are more acidic ($R_{CE/AE}$ < 1) than coarse particles ($R_{CE/AE}$ > 1) in Chengdu (Fig. 3). Since SO_4^{2-} and NO_3^- are dominant ions in $PM_{2.1}$, it is likely that the ambient NH_3 was insufficient to completely neutralize the H_2SO_4 and HNO_3 acids, despite the significantly high loading of NH_4^+. While in coarse particles, the SO_4^{2-}, Ca^{2+} and NO_3^- accounted for 76% of the total WSIIs, and the Ca^{2+} was excessive to integrate with the SO_4^{2-} and NO_3^- (He *et al.*, 2012; Chen *et al.*, 2015; Huang *et al.*, 2018). However, two anomalous high $R_{CE/AE}$ values (i.e., > 1) of fine particles were observed in May and July of 2012, when the $PM_{2.1}/PM_{11}$ ratios were high (Fig. 1), which can be ascribed to the influence from biomass burning episodes that contribute the large amount of cations (e.g., NH_4^+, K^+, and Na^+). The decrease trend of $R_{CE/AE}$ for fine particles from spring to winter was likely associated with the more intensive emission and conversion of anthropogenic acidic species (e.g., SO_2 and NO_x) (Kerminen *et al.*, 2001; Tian *et al.*, 2018).

Implications for SO_4^{2-} and NO_3^- Pollution

The A/S ratios in PM were found to be 1.79, 1.33, 1.19 and 1.14 in winter, spring, summer and autumn, respectively, at Chengdu. According to the threshold value of A/S (1.5) suggested by Pathak *et al.* (2004, 2009), it is clear that the "NH_3-rich" and "NH_3-poor" atmospheres prevailed in winter and all other three seasons, respectively. Hence, the NO_3^- in fine-mode particles at Chengdu should have been formed through heterogeneous reactions during spring to autumn. Whereas in winter, it might have been generated by homogeneous gas-phase reactions of HNO_3 with NH_3, because the rate may be much higher for the formation of NH_4NO_3 rather than the neutralization rate of H_2SO_4 by ambient NH_3 (Huang *et al.*, 2018; Tian *et al.*, 2018). Additionally, the size distribution of NO_3^- in Fig. 2(b) may be partially interpreted by the seasonal A/S values obtained, such as the minor coarse-mode peaks could be associated with $Ca(NO_3)_2$ or $Mg(NO_3)_2$, which were heterogeneously formed on pre-existed soil particles (Zhuang *et al.*, 1999; Li *et al.*, 2018).

We also calculated the $[NO_3^-]/[SO_4^{2-}]$ mass ratios in both fine and coarse fractions in each season. Their averages were generally less than 1 (Figs. 3(d)–3(e)), indicating higher contribution from stationary sources emissions than that from mobile sources at Chengdu (Yao *et al.*, 2002). Average coarse-mode $[NO_3^-]/[SO_4^{2-}]$ in warm seasons (i.e., 0.84 and 0.54 during spring and summer, respectively) were significantly higher than that of fine mode (0.43 and 0.27, respectively), but it was the opposite in cold seasons (0.59 and 0.68 in fine mode and 0.58 and 0.43 in coarse mode in

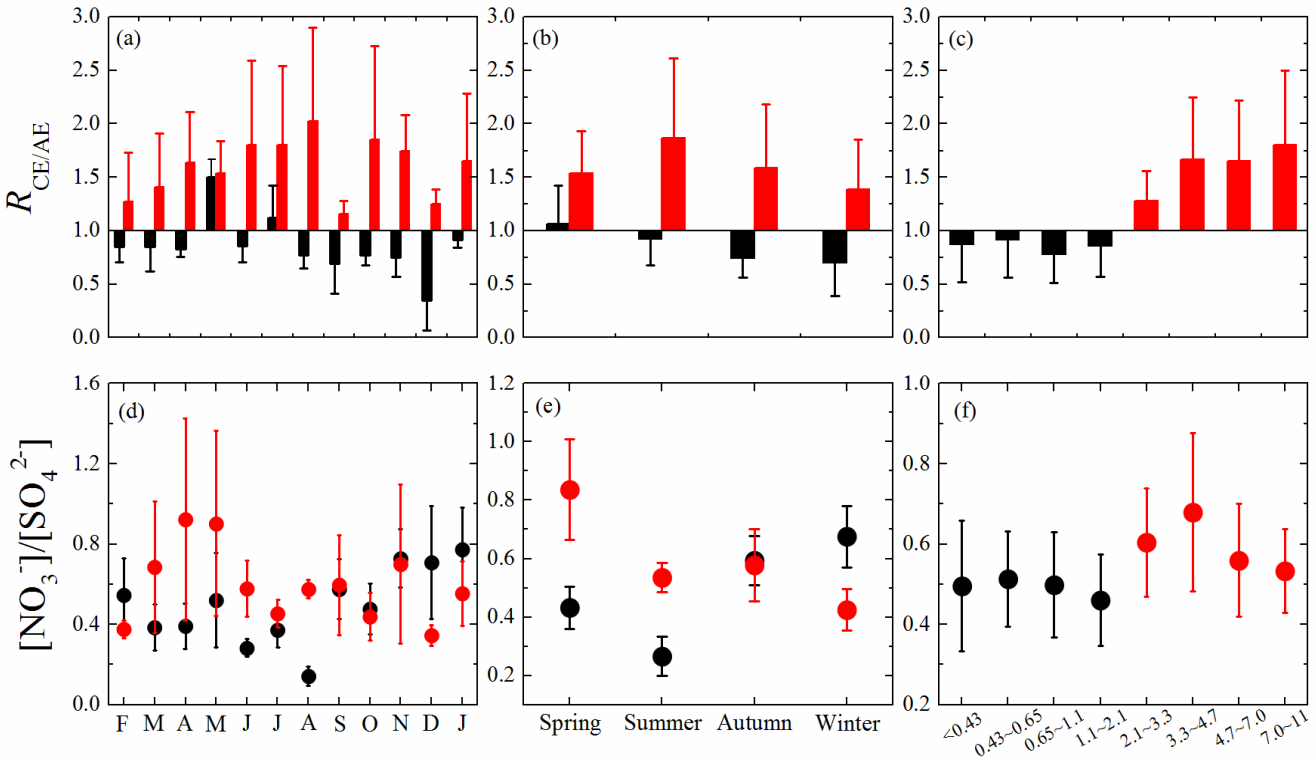

Fig. 3. The $R_{CE/AE}$ and $[NO_3^-]/[SO_4^{2-}]$ mass ratios in (a and d) different months and (b and e) seasons, and (c and f) size ranges, respectively (red for coarse-mode particles; black for fine-mode particles).

autumn and winter, respectively). Based on hourly measurements of acidic gases, ammonia and secondary inorganic aerosols in a tropical urban atmosphere, Behera *et al.* (2013) reported that the conversion of SO_2 into SO_4^{2-} and HNO_3 into NO_3^- was sensitive to the changes in temperature and relative humidity, respectively. However, due to the existence of thermodynamic equilibrium between precursor gases and fine particle NH_4^+ salts (e.g., NH_4NO_3), the conversion of HNO_3 into NO_3^- may also be sensitive to the changes in temperature, but the $Ca(NO_3)_2$ or $Mg(NO_3)_2$ in coarse mode were supposed to be less sensitive to the variations in the temperature (Zhuang *et al.*, 1999; Zhang *et al.*, 2008; He *et al.*, 2012). Moreover, the formation of aerosol NO_3^- could also be influenced by the ambient NH_3 content (Pathak *et al.*, 2004, 2009; Huang *et al.*, 2018). Therefore, we infer that the size and seasonal distributions of aerosol $[NO_3^-]/[SO_4^{2-}]$ at Chengdu were driven by the conversion of gaseous precursors and meteorological conditions (Zhuang *et al.*, 1999; Guo *et al.*, 2010; Huang *et al.*, 2016). Besides, the annual averages of fine-mode $[NO_3^-]/[SO_4^{2-}]$ were lower than that of coarse-mode particles (Fig. 3(f)), indicating the high abundance of coarse-mode NO_3^- and fine-mode SO_4^2 resulted due to the prevailing NH_3-poor atmosphere at Chengdu (Pathak *et al.*, 2009).

The scatter plots of the molar concentration of NO_3^- and NO_3^-/SO_4^{2-} (N/S) molar ratios as a function of A/S ratios in each season are illustrated in Fig. 4. Correlation between A/S and NO_3^- found to be positive and significant in spring ($p < 0.01$) and winter ($p < 0.01$). It implies that the formation of NO_3^- is increased with the increase of A/S. However, the molar concentrations of NO_3^- were comparable in each and every season, suggesting that NH_3 might have played a critical role in altering the heterogeneous and homogeneous formation process of aerosol NO_3^-, depending on NH_3-poor and -rich atmosphere, respectively (Pathak *et al.*, 2009; Huang *et al.*, 2018). This result is consistent with the results obtained by Weber *et al.* (2016) that the aerosol NH_4NO_3 concentrations increase with decreasing SO_4^{2-} in the steady-state NH_3 atmosphere of southeastern United States. Whereas the linear relations between A/S and N/S molar ratio were positive and negative in winter ($0.01 < p < 0.05$) and spring ($p < 0.001$), respectively (Fig. 4(b)). These relations together with the significant positive correlations between A/S and NO_3^- molar concentration in winter and spring (Fig. 4(a)) imply that the formation of NO_3^- was more influenced than that of SO_4^{2-} formation with the increase in A/S during winter, when the formation of $(NH_4)_2SO_4$ come to its limited regimes relative to the NH_3 content, yet the $HNO_{3(g)}$ become available for NH_3 to form the aerosol NO_3^- predominantly (Huang *et al.*, 2018; Tian *et al.*, 2018). In addition, the previous studies also indicated that the low temperature is favorable for the formation of NO_3^- but not for the SO_4^{2-} (Guo *et al.*, 2010; Huang *et al.*, 2016;). Thus, the formation of NO_3^- could be more efficient than SO_4^{2-} during cold and NH_3-rich atmosphere in winter.

In contrast, aerosol SO_4^{2-} might have more efficiently formed from homogeneous gas-phase reactions of H_2SO_4 and NH_3 than aerosol NO_3^- with the increase in A/S in spring in NH_3-poor and dry atmosphere (Table 1). It is likely

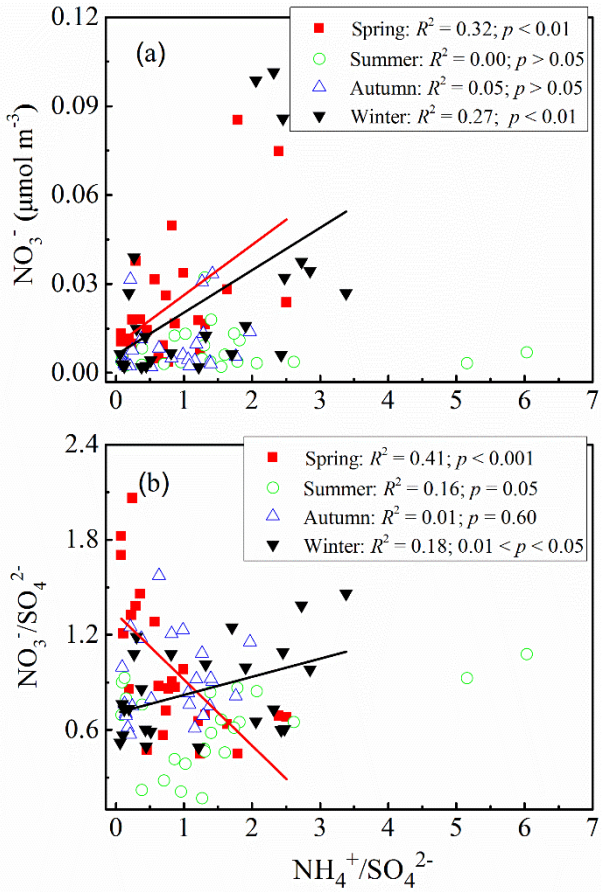

Fig. 4. Scatter plots of (a) NO_3^- molar concentration and (b) NO_3^-/SO_4^{2-} molar ratios as a function of NH_4^+/SO_4^{2-} molar ratios over the four sampling seasons (n = 24 for each season).

because the kinetic rate of neutralization of H_2SO_4 by NH_3 could be significantly higher than forming aerosol NO_3^- in NH_3-poor atmosphere (Huang *et al.*, 2018), whereas the NO_3^- formation could occur from the hydrolysis of N_2O_5 under high relative humidity (Pathak *et al.*, 2009). Furthermore, the low relative humidity in spring might have promoted the heterogeneous reaction of HNO_3 on soil dust particles, one of the formation pathways of aerosol NO_3^-, at Chengdu (Pathak *et al.*, 2011). According to the lower A/S (< 1.5) and higher $R_{CE/AE}$ (> 1) values, the nonvolatile cations from minerals could have played a vital role in forming the particles in spring at Chengdu, and this can also be evidenced by the $PM_{2.1}/PM_{11}$ ratio shows in Fig. 1. In Fig. 3(e), as the coarse-mode N/S is significantly higher than fine-mode particles in spring, the NO_3^- were supposed to be formed on the minerals, through heterogeneous reactions, and mainly in the forms of $Mg(NO_3)_2$ or $Ca(NO_3)_2$. Otherwise, only several minor peaks for SO_4^{2-} are shown in coarse mode, while the fine-mode SO_4^{2-} is likely to be formed more efficiently than NO_3^- in spring with the increase in A/S (Fig. 4). On the other hand, the correlations are insignificant in summer and winter, and this might principally be ascribed to the high rainfall, which greatly impacts the WSII loading in the atmosphere (Pan *et al.*, 2017).

CONCLUSIONS

The characteristics of WSIIs in size-segregated particles in urban Chengdu were investigated over a one-year period. The results showed that the WSIIs were more enriched in the fine particles than the coarse ones, and NH_4^+, SO_4^{2-}, and NO_3^-, the dominant WSIIs in the fine fraction, were mostly generated by the conversion of anthropogenic gaseous precursors, especially during the cold seasons. The calculated equivalent ratios ($R_{CE/AE}$) indicated that the fine particles were more acidic (< 1) than the coarse particles (> 1). Furthermore, the NH_4^+/SO_4^{2-} (A/S) molar ratio in the fine-mode PM suggested that the atmosphere was NH_3-poor during spring, summer, and autumn but NH_3-rich during winter; therefore, the NO_3^- in the fine fraction was formed homogeneously during winter and heterogeneously during the other three seasons. Based on the positive correlations between the A/S and NO_3^- molar concentrations observed during spring and winter, the increase in NH_3 or NH_4^+ may enhance the formation of NO_3^- in aerosols, but certain meteorological conditions, such as high temperatures and concentrated rainfall, significantly disrupt this relationship. Finally, we infer from the seasonal correlations between the A/S and NO_3^-/SO_4^{2-} molar ratios in addition to the temporal variation in the NO_3^-/SO_4^{2-} molar ratio that the NH_3-rich atmosphere during winter favors the formation of NO_3^- rather than SO_4^{2-}, whereas the NH_3-poor atmosphere during spring favors the formation of the latter, as the heterogeneous formation of the former during this season is less efficient.

ACKNOWLEDGEMENTS

This work was supported by the National Natural Science Foundation of China (Grant No. 41173022 and 41773006) and Natural Science Foundation of Tianjin (Grant No. 17JCZDJC39400). We also appreciate Ph.D. Jing Yu and Long Lv for helping field particulate matter sampling.

REFERENCES

Behera, S.N., Betha, R. and Balasubramanian, R. (2013). Insights into chemical coupling among acidic gases, ammonia and secondary inorganic aerosols. *Aerosol Air Qual. Res.* 13: 1282–1296.

Carpenter, R. (1969). Factors controlling the marine geochemistry of fluorine. *Geochim. Cosmochim. Acta* 33: 1153–1167.

Chen, Y. and Xie, S.D. (2013). Long-term trends and characteristics of visibility in two megacities in southwest China: Chengdu and Chongqing. *J. Air Waste Manage. Assoc.* 63: 1058–1069.

Chen, Y. and Xie, S.D. (2014). Characteristics and formation mechanism of a heavy air pollution episode caused by biomass burning in Chengdu, Southwest China. *Sci. Total Environ.* 473–474: 507–517.

Chen, Y., Luo, B. and Xie, S.D. (2015). Characteristics of the long-range transport dust events in Chengdu, Southwest China. *Atmos. Environ.* 122: 713–722.

Dockery, D.W., Pope, C.A., Xu, X., Spengler, J.D., Ware, J.H., Fay, M.E., Ferris, B.G. Jr. and Speizer, F.E. (1993). An association between air pollution and mortality in six U. S. cities. *N. Engl. J. Med.* 329: 1753–1759.

Guo, S., Hu, M., Wang, Z.B., Slanina, J. and Zhao, Y.L. (2010). Size-resolved aerosol water-soluble ionic compositions in the summer of Beijing: Implication of regional secondary formation. *Atmos. Chem. Phys.* 10: 947–959.

He, K., Zhao, Q., Ma, Y., Duan, F., Yang, F., Shi, Z. and Chen, G. (2012). Spatial and seasonal variability of $PM_{2.5}$ acidity at two Chinese megacities: Insights into the formation of secondary inorganic aerosols. *Atmos. Chem. Phys.* 12: 1377–1395.

Hennigan, C.J., Izumi, J., Sullivan, A.P., Weber, R.J. and Nenes, A. (2015). A critical evaluation of proxy methods used to estimate the acidity of atmospheric particles. *Atmos. Chem. Phys.* 15: 2775–2790.

Huang, R.J., Zhang, Y., Bozzetti, C., Ho, K.F., Cao, J.J., Han, Y., Daellenbach, K.R., Slowik, J.G., Platt, S.M., Canonaco, F., Zotter, P., Wolf, R., Pieber, S.M., Bruns, E.A., Crippa, M., Ciarelli, G., Piazzalunga, A., Schwikowski, M., Abbaszade, G., Schnelle-Kreis, J., Zimmermann, R., An, Z., Szidat, S., Baltensperger, U., El Haddad, I. and Prévôt, A.S. (2014). High secondary aerosol contribution to particulate pollution during haze events in China. *Nature* 514: 218–222.

Huang, X., Liu, Z., Zhang, J., Wen, T., Ji, D. and Wang, Y. (2016). Seasonal variation and secondary formation of size-segregated aerosol water-soluble inorganic ions during pollution episodes in Beijing. *Atmos. Res.* 168: 70–79.

Huang, X., Zhang, J., Luo, B., Wang, L., Tang, G., Liu, Z., Song, H., Zhang, W., Yuan, L. and Wang, Y. (2018). Water-soluble ions in $PM_{2.5}$ during spring haze and dust periods in Chengdu, China: Variations, nitrate formation and potential source areas. *Environ Pollut.* 243: 1740–1749.

IPCC (2013). Climate Change 2013: The Physical Science Basis. Contribution of Working Group I to the Fifth Assessment Report of the Intergovernmental Panel on Climate Change, Stocker, T.F., Qin, D., Plattner, G.K., *et al.* (Eds.), Cambridge University Press, doi: 10.1017/CBO9781107415324.016.

Jayarathne, T., Stockwell, C.E., Yokelson, R.J., Nakao, S. and Stone, E. (2014). Emissions of Fine Particle Fluoride from Biomass Burning. *Environ. Sci. Technol.* 48: 12636–12644.

Jiang, F., Liu, F., Lin, Q., Fu, Y., Yang, Y., Peng, L., Lian, X., Zhang, G., Bi, X., Wang, X. and Sheng, G. (2019). Characteristics and formation mechanisms of sulfate and nitrate in size-segregated atmospheric particles from urban Guangzhou, China. *Aerosol Air Qual. Res.* 19: 1284–1293

Kalinić, N., Vağić, V., Hršak, J. and Lambaša-Belak, Ž. (1997). Fluoride mass concentrations in the air at different distances from an aluminum factory. *Environ. Res. Forum.* 7–8: 253–257.

Kerminen, V.M., Hillamo, R., Teinilä, K., Pakkanen, T., Allegrini, I. and Sparapani, R. (2001). Ion balances of size-resolved tropospheric aerosol samples: Implications for the acidity and atmospheric processing of aerosols.

Atmos. Environ. 35: 5255–5265.

Klimont, Z., Kupiainen, K., Heyes, C., Purohit, P., Cofala, J., Rafaj, P., Borken-Kleefeld, J. and Schöpp, W. (2017). Global anthropogenic emissions of particulate matter including black carbon. *Atmos. Chem. Phys.* 17: 8681–8723.

Kulmala, M., Vehkamäki, H., Petäjä, T., Dal Maso, M., Lauri, A., Kerminen, V.M., Birmili, W. and McMurry, P.H. (2004). Formation and growth rates of ultrafine atmospheric particles: A review of observations. *J. Aerosol Sci.* 35: 143–176.

Li, W.J. and Shao, L.Y. (2009). Observation of nitrate coatings on atmospheric mineral dust particles. *Atmos. Chem. Phys.* 9: 1863–1871.

Li, X.D., Yang, Z., Fu, P., Yu, J., Lang, Y.C., Liu, D., Ono, K. and Kawamura, K. (2015). High abundances of dicarboxylic acids, oxocarboxylic acids, and α-dicarbonyls in fine aerosols ($PM_{2.5}$) in Chengdu, China during wintertime haze pollution. *Environ. Sci. Pollut. Res.* 22: 12902–12918.

Li, Y., Hao, Q., Wen, T., Ji, D., Liu, Z., Wang, Y., Li, X., He, X. and Jiang, C. (2018). Pollution characteristics of water-soluble ions in aerosols in the urban area in Beibei of Chongqing. *Aerosol Air Qual. Res.* 18: 1531–1544.

Lin, Y.C., Cheng, M.T., Ting, W.Y. and Yeh, C.R. (2006). Characteristics of Gaseous HNO_2, HNO_3, NH_3 and particulate ammonium nitrate in an urban city of central Taiwan. *Atmos. Environ.* 40: 4725–4733.

Lin, Y.C. and Cheng, M.T. (2007). Evaluation of formation rates of NO_2 to gaseous and particulate nitrate in the urban atmosphere. *Atmos. Environ.* 41: 1903–1910.

Liu, X., Sun, K., Qu, Y., Hu, M., Sun, Y., Zhang, F. and Zhang, Y. (2015). Secondary formation of sulfate and nitrate during a haze episode in megacity Beijing, China. *Aerosol Air Qual. Res.* 15: 2246–2257.

Ning, G., Wang, S., Yim, S.H.L., Li, J., Hu, Y., Shang, Z., Wang, J. and Wang, J. (2018). Impact of low-pressure systems on winter heavy air pollution in the northwest Sichuan Basin, China. *Atmos. Chem. Phys*. 18: 13601–13615.

Pan, Y.P., Zhu, X.Y., Tian, S.L., Wang, L.L., Zhang, G.Z., Zhou, Y.B., Xu, P., Hu, B. and Wang, Y.S. (2017). Wet deposition and scavenging ratio of air pollutants during an extreme rainstorm in the north china plain. *Atmos. Oceanic Sci. Lett*. 10: 348–353.

Pathak, R.K., Yao, X.H. and Chan, C.K. (2004). Sampling artifacts of acidity and ionic species in $PM_{2.5}$. *Environ. Sci. Technol.* 38: 254–259.

Pathak, R.K., Wu, W.S. and Wang, T. (2009). Summertime $PM_{2.5}$ ionic species in four major cities of China: Nitrate formation in an ammonia-deficient atmosphere. *Atmos. Chem. Phys.* 9: 1711–1722.

Pathak, R.K. Wang, T. and Wu, W.S. (2011). Nighttime enhancement of $PM_{2.5}$ nitrate in ammonia-poor atmospheric conditions in Beijing and Shanghai: Plausible contributions of heterogeneous hydrolysis of N_2O_5 and HNO_3 partitioning. *Atmos. Environ.* 45: 1183–1191.

Shi, G.L., Tian, Y.Z., Ma, T., Song, D.L., Zhou, L.D., Han, B., Feng, Y.C. and Russell, A.G. (2017). Size distribution, directional source contributions and pollution status of PM from Chengdu, China during a long-term sampling campaign. *J. Environ. Sci. (China)* 56: 1–11.

Seinfeld, J.H. and Pandis, S.N. (1998). *Atmospheric chemistry and physics: From air pollution to climate change.* John Wiley & Sons, Inc., New York, USA.

Tao, J., Zhang, L., Engling, G., Zhang, R., Yang, Y., Cao, J., Zhu, C., Wang, Q. and Luo, L. (2013). Chemical composition of $PM_{2.5}$ in an urban environment in Chengdu, China: Importance of springtime dust storms and biomass burning. *Atmos. Res.* 122: 270–283.

Tao, J., Gao, J., Zhang, L., Zhang, R., Che, H., Zhang, Z., Lin, Z., Jing, J., Cao, J. and Hsu, SC. (2014). $PM_{2.5}$ pollution in a megacity of southwest China: Source apportionment and implication. *Atmos. Chem. Phys.* 14: 8679–8699.

Tian, S.L., Pan, Y.P. and Wang, Y.S. (2018). Ion balance and acidity of size-segregated particles during haze episodes in urban Beijing. *Atmos. Res.* 201: 159–167.

Tian, Y.Z., Wu, J.H., Shi, G.L., Wu, J.Y., Zhang, Y.F., Zhou, L.D., Zhang, P. and Feng, Y.C. (2013). Long-term variation of the levels, compositions and sources of size-resolved particulate matter in a megacity in China. *Sci. Total Environ.* 463–464: 462–468.

Tian, Y.Z., Shi, G.L., Huang-Fu, Y.Q., Song, D.L., Liu, J.Y., Zhou, L.D. and Feng, Y.C. (2016) Seasonal and regional variations of source contributions for PM_{10} and $PM_{2.5}$ in urban environment. *Sci. Total Environ.* 557–558: 697–704.

Vieira-Filho, M., Pedrotti, J.J. and Fornaro, A. (2016). Water-soluble ions species of size-resolved aerosols: Implications for the atmospheric acidity in São Paulo megacity, Brazil. *Atmos. Res.* 181: 281–287.

Wang, G., Zhang, R., Gomez, M.E., Yang, L., Levy Zamora, M., Hu, M., Lin, Y., Peng, J., Guo, S., Meng, J., Li, J., Cheng, C., Hu, T., Ren, Y., Wang, Y., Gao, J., Cao, J., An, Z., Zhou, W., Li, G., Wang, J., Tian, P., Marrero-Ortiz, W., Secrest, J., Du, Z., Zheng, J., Shang, D., Zeng, L., Shao, M., Wang, W., Huang, Y., Wang, Y., Zhu, Y., Li, Y., Hu, J., Pan, B., Cai, L., Cheng, Y., Ji, Y., Zhang, F., Rosenfeld, D., Liss, P.S., Duce, R.A., Kolb, C.E. and Molina, M.J. (2016). Persistent sulfate formation from London Fog to Chinese haze. *Proc. Natl. Acad. Sci. U.S.A.* 113: 13630–13635.

Wang, J., Hu, Z., Chen, Y., Chen, Z. and Xu, S. (2013a). Contamination characteristics and possible sources of PM_{10} and $PM_{2.5}$ in different functional areas of Shanghai, China. *Atmos. Environ.* 68: 221–229.

Wang, J., Zhang, J.S., Liu, Z.J., Wu, J.H., Zhang, Y.F., Han, S.Q., Zheng, X.J., Zhou, L.D., Feng, Y.C. and Zhu, T. (2017a). Characterization of chemical compositions in size-segregated atmospheric particles during severe haze episodes in three mega-cities of China. *Atmos. Res.* 187: 138–146.

Wang, L., Ji, D., Li, Y., Gao, M., Tian, S., Wen, T., Liu, Z., Wang, L., Xu, P., Jiang, C. and Wang, Y. (2017b). The impact of relative humidity on the size distribution and chemical processes of major water-soluble inorganic ions in the megacity of Chongqing, China. *Atmos. Res.* 192:

19–29.

Wang, P., Cao, J., Tie, X., Wang, G., Li, G., Hu, T., Wu, Y., Xu, Y., Xu, G., Zhao, Y., Ding, W., Liu, H. and Huang, R. (2015). Impact of meteorological parameters and gaseous pollutants on $PM_{2.5}$ and PM_{10} mass concentrations during 2010 in Xi'an, China. *Aerosol Air Qual. Res.* 15: 1844–1854.

Wang, Q., Cao, J., Shen, Z., Tao, J., Xiao, S., Luo, L., He, Q. and Tang, X. (2013b). Chemical characteristics of $PM_{2.5}$ during dust storms and air pollution events in Chengdu, China. *Particuology* 11: 70–77.

Wang, S., Yu, S., Yan, R., Zhang, Q., Li, P., Wang, L., Liu, W. and Zheng, X. (2017c). Characteristics and origins of air pollutants in Wuhan, China, based on observations and hybrid receptor models. *J. Air Waste Manage. Assoc.* 67: 739–753.

Wang, X., Bi, X., Sheng, G. and Fu, J. (2006). Chemical composition and sources of PM_{10} and $PM_{2.5}$ aerosols in Guangzhou, China. *Environ. Monit. Assess.* 119: 425–439.

Wang, Y., Zhuang, G.S., Tang, A., Yuan, H., Sun, Y.L., Chen, S. and Zhang, A. (2005). The ion chemistry and the source of $PM_{2.5}$ aerosol in Beijing. *Atmos. Environ.* 39: 3771–3784.

Weber, R.J., Guo, H., Russell, A.G. and Nenes, A. (2016). High aerosol acidity despite declining atmospheric sulfate concentrations over the past 15 years. *Nat. Geosci.* 9: 282–285.

West, J.J., Cohen, A., Dentener, F., Brunekreef, B., Zhu, T., Armstrong, B., Bell, M.L., Brauer, M., Carmichael, G., Costa, D.L., Dockery, D.W., Kleeman, M., Krzyzanowski, M., Künzli, N., Liousse, C., Lung, S.C., Martin, R.V., Pöschl, U., Pope, C.A., Roberts, J.M., Russell, A.G. and Wiedinmyer, C. (2016). What we breathe impacts our health: Improving understanding of the link between air pollution and health. *Environ. Sci. Technol.* 50: 4895–4904.

WHO (2006). WHO Air quality guidelines for particulate matter, ozone, nitrogen dioxide and sulfur dioxide: Global update 2005: Summary of risk assessment. No. WHO/SDE/PHE/OEH/06.02. World Health Organization, Geneva.

WHO (2013). Review of evidence on health aspects of air pollution-REVIHAAP Project. World Health Organization, WHO Regional Office for Europe, Copenhagen.

Wu, P., Huang, X., Zhang, J., Luo, B., Luo, J., Song, H., Zhang, W., Rao, Z., Feng, Y. and Zhang, J. (2018). Characteristics and formation mechanisms of autumn haze pollution in Chengdu based on high time-resolved water-soluble ion analysis. *Environ. Sci. Pollut. Res.* 26: 2649–2661.

Wu, X., Deng, J., Chen, J., Hong, Y., Xu, L., Yin, L., Du, W., Hong, Z., Dai, N. and Yuan, C.S. (2017). Characteristics of water-soluble inorganic components and acidity of $PM_{2.5}$ in a coastal city of China. *Aerosol Air Qual. Res.* 17: 2152–2164.

Xiao, H.Y. and Liu, C.Q. (2004). Chemical characteristics of water-soluble components in TSP over Guiyang, SW China. *Atmos. Environ.* 38: 6297–6306.

Yang, Z., Li, X.D., Deng, J. and Wang, H.Y. (2015). Stable sulfur isotope ratios and water-soluble inorganic compositions of PM_{10} in Yichang City, central China. *Environ. Sci. Pollut. Res. Int.* 22: 13564–13572.

Yao, L., Garmash, O., Bianchi, F., Zheng, J., Yan, C., Kontkanen, J., Junninen, H., Mazon, S.B., Ehn, M., Paasonen, P. and Sipilä, M. (2018). Atmospheric new particle formation from sulfuric acid and amines in a Chinese megacity. *Science* 361: 278–281.

Yao, X., Chan, C.K., Fang, M., Cadle, S., Chan, T., Mulawa, P., He, K. and Ye, B. (2002). The water-soluble ionic composition of $PM_{2.5}$ in Shanghai and Beijing, China. *Atmos. Environ.* 36: 4223–4234.

Zhang, L., Vet, R., Wiebe, A., Mihele, C., Sukloff, B., Chan, E., Moran, M.D. and Iqbal, S. (2008). Characterization of the size-segregated water-soluble inorganic ions at eight Canadian rural sites. *Atmos. Chem. Phys.* 8: 7133–7151.

Zhang, R., Wang, G., Guo, S., Zamora, M.L., Ying, Q., Lin, Y., Wang, W., Hu, M. and Wang, Y. (2015). Formation of urban fine particulate matter. *Chem. Rev.* 115: 3803–3855.

Zhao, J., Zhang, F., Xu, Y. and Chen, J. (2011). Characterization of water-soluble inorganic ions in size-segregated aerosols in coastal city, Xiamen. *Atmos. Res.* 99: 546–562.

Zhuang, H., Chan, C.K., Fang, M. and Wexler, A.S. (1999). Formation of nitrate and non-sea-salt sulfate on coarse particles. *Atmos. Environ.* 33: 4223–4233.

Zou, J., Liu, Z., Hu, B., Huang, X., Wen, T., Ji, D., Liu, J., Yang, Y., Yao, Q. and Wang, Y. (2018). Aerosol chemical compositions in the North China Plain and the impact on the visibility in Beijing and Tianjin. *Atmos. Res.* 201: 235–246.

Received for review, July 29, 2019
Revised, November 9, 2019
Accepted, November 10, 2019